

CFD Study of Isothermal Ablation

D. Bianchi, E. Martelli, F. Nasuti and M. Onofri
Sapienza University of Rome, Dipartimento di Meccanica e Aeronautica
Via Eudossiana 18, I-00184 Rome, Italy

Abstract

CFD codes typically treat fluid/solid boundary conditions in a simplified manner such as constant prescribed temperature or heat flux with zero mass transfer. However, thermal protection materials (TPS) strongly interact with the flow so that simple CFD surface boundary conditions cannot realistically be used for TPS design. In order to obtain a better estimation of the wall heat flux over an ablating surface, a two-dimensional axisymmetric full Navier-Stokes equation solver is used coupled with surface mass balance and an equilibrium ablation model for graphite. The effect of gas injection in the boundary layer is studied focusing the attention on the wall heat flux and its reduction due to convective blockage. Flat plate tests are presented. Results are compared with the most commonly used simplified approaches.

Nomenclature

B'	normalized mass blowing rate
C_h	Stanton number for heat transfer
C_m	Stanton number for mass transfer
D	diffusion coefficient
h	enthalpy
j	diffusive mass flux
k	thermal conductivity
Le	<i>Lewis</i> number
M	<i>Mach</i> number
\dot{m}	blowing mass rate per unit area
N_c	number of species
N_{el}	number of elements
N_r	number of surface reactions
p	pressure
q_{cond}	heat conduction into the solid
q_{rad}	radiative flux to the surface
T	temperature
u	streamwise velocity
v	velocity component normal to surface
y	mass fraction
α_{ki}	mass fraction of element k in species i
ϵ	surface emissivity
η	outward coordinate normal to surface
λ	blowing correction parameter
ρ	density
σ	Stefan-Boltzmann constant
ω	mass flux due to surface chemical reaction
<i>Subscript</i>	
e	outer edge of boundary layer or freestream
i	species
k	element
s	solid properties at gas-solid interface
w	gas properties at gas-solid interface

1. Introduction

Upon exposure to ballistic re-entry and rocket nozzle environments, heat-protection materials are subjected to severe thermal and mechanical conditions. Various thermal protection systems (heat sink, transpiration cooling, ablation) have been proposed and investigated quite extensively, especially from the experimental viewpoint. Among them, ablative thermal protection systems (TPS), which are characterized by the sacrificial removal of the surface material for the protection of the underlying structure, have been widely applied to re-entry vehicles and solid rocket nozzles. Ablative TPS must be designed to keep the excessive heat from damaging the vehicle or its contents with a minimum weight penalty.

There are two categories of ablative TPS: the *charring* and the *non-charring* ablators. *Charring* TPS materials are made of a filler (usually a resin) and a reinforcing material (usually carbon). When heated, the resin experiences a series of chemical reactions that release gaseous by products (pyrolysis) leaving a layer of *char* or residue. Gas pressure in the pyrolysis zone forces the pyrolysis gas to flow through the *char* into the boundary layer. The *char* itself can recede due to chemical or mechanical action by the boundary layer. For a *non-charring* ablator (such as carbon-carbon), mass loss occurs only by surface ablation and mechanical erosion. Both the *charring* and *non-charring* ablators sacrifice some TPS material to divert the energy that would otherwise enter the vehicle.

An accurate prediction of the thermal response of these materials is essential to successfully carry out the design of an optimum TPS. In recent years, computational fluid dynamics (CFD) technology has continued to develop in the areas of non-equilibrium flow, multispecies kinetics, and multidimensional full Navier-Stokes capabilities. However, most codes use primitive surface boundary conditions and cannot be realistically used to predict the aerothermal heating for the design of TPS.¹ In fact, CFD codes typically treat fluid/solid boundary conditions in a simplified manner and mass transfer is often not considered. Current methods focus their attention on some aspects of the problem at the expense of others. Thus aerodynamic methods concentrate on the flowfield, and rely on other methods to provide material-response characteristics; on the other hand, material-response methods concentrate on surface ablation and heat conduction in the material, using simplified models to provide the aerothermodynamic heating. However, in reality all these phenomena are highly coupled. Thus, in order to improve estimating of the heat flux over an ablating surface, a flow solver with ablating surface conditions becomes a requirement. This goal can be achieved by considering that the surface energy and mass balances, coupled with an ablation model, provide complete thermochemical boundary conditions for a solution of the fully coupled fluid-dynamics/solid-mechanics problem.²

In this study, a general surface boundary condition with mass balance and surface thermochemistry effects is developed for equilibrium gas states adjacent to a *non-charring* (graphite) ablating surface. Based on this formulation, a surface thermochemistry procedure is developed and integrated with a multi-species reacting Navier-Stokes solver.

2. Physical and mathematical modeling

The physics of the hot-gases over a solid surface is modeled by the multispecies reacting Navier-Stokes governing equations, which are solved by a code^{3,4} based on the lambda scheme.⁵ Because of the chemically active surface, further physical modeling is necessary for the fluid-surface interaction. The latter aspect requires the addition of a mathematical model of the hot-gas-flow boundary condition which describes the physics of the surface phenomena.

2.1 Ablating surface boundary conditions

The general boundary conditions for a chemically reacting, *non-charring* ablating surface can be written as^{1,2}:

$$k \left. \frac{\partial T}{\partial \eta} \right|_w + \sum_i^{N_c} h_i \rho D \left. \frac{\partial y_i}{\partial \eta} \right|_w + q_{rad} = (\rho v) h_w - \dot{m} h_s + \epsilon \sigma T^4 + q_{cond} \quad (1)$$

which is the surface energy balance (SEB), and:

$$\rho D \left. \frac{\partial y_i}{\partial \eta} \right|_w = (\rho v) y_{w,i} - \dot{m} y_{s,i} + \sum_r^{N_r} \omega_i^r \quad i = 1, N_c \quad (2)$$

which is the surface mass balance (SMB) for the i^{th} species. The subscripts w and s denote gas and solid properties at the wall, respectively.

The terms on the left-end side of Eq.(1) are the heat fluxes entering the surface due to conduction, diffusion and radiation from the gas to the surface, while the terms of the right-end side are the heat fluxes leaving the surface due to blowing, surface ablation, re-radiation, and conduction in the material. The conduction term q_{cond} is an input for

the CFD analysis, which has to be provided by numerical or semi-analytic CSM (Computational Solid Mechanics) computation.

The term on the left-end side of Eq.(2) is the mass flux entering the surface due to diffusion, while the terms on the right-end side are the mass fluxes leaving the surface due to blowing, surface ablation, and surface reactions (different from ablation, i.e. catalysis). The term ω_i^r is the mass flux of species i due to surface reaction r , and $y_{s,i}$ is the mass of species i produced or consumed in the ablation process per mass of TPS material ablated, i.e. $y_{s,i} = \dot{m}_i/\dot{m}$. The $y_{s,i}$ are positive for ablation products, negative for species which are consumed in the ablation process and sum to unity. Eq.(1) and (2) can also be applied to a non-ablating surface, with $\dot{m} = 0$. A summation of Eq.(2) over all the species, considering that the summation made over the diffusive and chemical terms is zero because of mass conservation, yields:

$$(\rho v) = \dot{m} \quad (3)$$

which can be used to simplify Eq.(1) and (2). It is interesting to note that a suitable combination of Eq.(1) and (2) allows to express the so-called *heat of ablation* term. This can be obtained by multiplying Eq.(2) for h_i and summing over all the species:

$$\sum_i^{N_c} h_i \rho D \left. \frac{\partial y_i}{\partial \eta} \right|_w = \dot{m} \left(\sum_i^{N_c} h_i y_{w,i} - \sum_i^{N_c} h_i y_{s,i} \right) + \sum_i^{N_c} \sum_r^{N_r} h_i \omega_i^r \quad (4)$$

The term $\sum_i \sum_r h_i \omega_i^r$ is the chemical energy flux due to surface reactions different from ablation. Substituting Eq.(4) into Eq.(1) and noting that the term $\sum_i h_i y_{w,i}$ is the enthalpy of the mixture of gases at wall h_w , yields:

$$k \left. \frac{\partial T}{\partial \eta} \right|_w + \sum_i^{N_c} \sum_r^{N_r} h_i \omega_i^r - \dot{m} \left(\sum_i^{N_c} h_i y_{s,i} - h_s \right) + q_{rad} = \epsilon \sigma T^4 + q_{cond} \quad (5)$$

The term $H_{abl} = \sum_i h_i y_{s,i} - h_s$ is the so-called heat of ablation, which is the difference between the enthalpies of the species created or consumed by the ablation mechanism and the enthalpy of the solid material at the surface temperature; therefore it represents the energy absorbed (or released) by the thermochemical ablation process. The term $\sum_i \sum_r h_i \omega_i^r - \dot{m} \cdot H_{abl}$ is therefore the heat flux due to the surface chemical reactions which will be referred to as *chemical heat flux*.

2.2 Surface Equilibrium assumption

For an ablating surface, the SMB takes different forms depending on whether or not the flow is in chemical equilibrium with the solid phase. For equilibrium flow, it is convenient to use elemental mass fraction y_k , which are known for the TPS material and which are variables in the CFD solutions. y_k represents the total mass fraction of element k independent of molecular configuration, i.e. $y_k = \sum_i \alpha_{ki} y_i$.

A summation of Eq.(2) over all the species yields a balance equation for each element k , and consequently eliminates the surface reaction term:

$$\rho D \sum_i^{N_c} \alpha_{ki} \left. \frac{\partial y_i}{\partial \eta} \right|_w = \dot{m} \sum_i^{N_c} \alpha_{ki} (y_{w,i} - y_{s,i}) \quad \Rightarrow \quad \rho D \left. \frac{\partial y_k}{\partial \eta} \right|_w = \dot{m} (y_{w,k} - y_{s,k}) \quad k = 1, N_{el} \quad (6)$$

The term $y_{w,k}$ is the elemental mass fraction of the gaseous mixture at the wall while $y_{s,k}$ is the mass of element k produced in the ablation process per mass of TPS material ablated, i.e. $y_{s,k} = \dot{m}_k/\dot{m}$. Clearly the $y_{s,k}$ must be equal to the elemental composition of the TPS material. The use of Eq.(6) together with the assumption of chemical equilibrium at wall permits to bypass the entire discussion about reaction mechanisms and the associated reaction rates, especially for the complex flowfields with ablation. The term $y_{s,k}$ only depends on the material composition while its species' counterpart, the term $y_{s,i}$, also depends on the reaction mechanism with the atmosphere.

The surface equilibrium approach provides satisfactory accuracy with reduced computational cost, although ablating surface non-equilibrium should be taken into account. However, only few data are available to validate gas-surface kinetic models which strongly affect the prediction of mass blowing rate.⁶ For these reasons the surface equilibrium approach has been used here: this is equivalent to assume that the regime is always diffusion controlled.

2.3 Ablation model

Solving the mass and energy surface balances is only possible if the ablation term is suitably modeled. Thus it is necessary to prescribe some relationships among the blowing mass flow rate \dot{m} and the flow and surface properties. Two different ablation models have been considered in the present study: a classical *thermochemical table model* and a *fully-coupled ablation model*. Both models rely on the assumption of surface equilibrium.

2.3.1 Thermochemical table model

The *thermochemical table* ablation models,⁷ which are the most widely used for TPS materials, are obtained from a solution of the equations for thermodynamic equilibrium between the TPS material and the atmosphere of interest, coupled with surface mass balance and simplified boundary-layer transfer potential methodology. With the transfer coefficient approach the diffusional mass flux of the i^{th} species to the surface can be expressed as:

$$\rho D \left. \frac{\partial y_i}{\partial \eta} \right|_w = \rho_e u_e C_m (y_{e,i} - y_{w,i}) \quad i = 1, N_c \quad (7)$$

where C_m is a dimensionless mass transfer coefficient and $(\)_e$ refers to the edge of the boundary layer. Substituting Eq.(7) in the mass balance Eq.(6) and introducing the dimensionless mass flux $B' = \dot{m}/\rho_e u_e C_m$, yields:

$$y_{e,k} + B' y_{s,k} = (1 + B') y_{w,k} \quad k = 1, N_{el} \quad (8)$$

For each value of B' , Eq.(8) permits to find the wall elemental composition ($y_{e,k}$ and $y_{s,k}$ are known). Once the $y_{w,k}$ are known, the wall temperature can be determined by the wall pressure and the assumption of chemical equilibrium using a free energy minimization procedure.⁸ The net result of the calculations is a set of thermochemical tables relating surface temperature and pressure to a dimensionless ablation mass flux.

Figure 1 shows $B'(T, p)$ for thermochemical ablation of carbon in air. At each pressure and temperature corresponds a dimensionless mass flux (left) and a mixture composition in equilibrium with the solid phase (right). As the pressure is increased, a higher surface temperature is needed to reach the same dimensionless ablation rate.

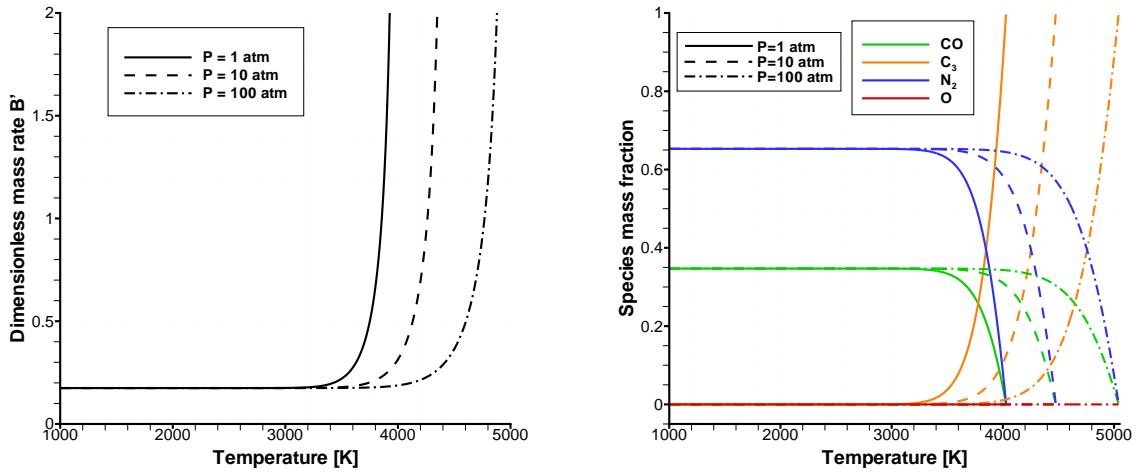


Figure 1: Dimensionless ablation rate $B'(T, P)$ (left) and wall composition (right) for carbon ablation in air.

The advantage of using these tables is that, once they have been generated, they are applicable over a wide range of aerothermal heating conditions. The disadvantage is that they are obtained with a very simplified boundary layer approach based on transfer coefficients to model species diffusion across the boundary-layer. From the definition of B' it is clear that the diffusion coefficient C_m plays a dominant role in determining the surface ablation rate, and thus the uncertainty in this estimated mass blowing rate can be high.

2.3.2 Fully-coupled ablation model

An accurate evaluation of the mass transfer mechanism is a key issue to predict the correct mass blowing rate and consequently the heat flux over an ablating surface; thus, a full Navier-Stokes approach is needed to solve the coupled material/flow problem: the advantage of using pre-generated $B'(T, P)$ tables is lost but the simplified boundary-layer transfer coefficient approach can be completely removed.

Assuming surface equilibrium, with the pressure coming from the flowfield and with the wall temperature assigned, the chemical composition at wall can be obtained. From these data the wall elemental composition is easily obtained and, as a consequence, also the wall diffusive mass flux of element k :

$$j_{w,k} = \rho D \left. \frac{\partial y_k}{\partial \eta} \right|_w = \sum_i \alpha_{ki} \rho D \left. \frac{\partial y_i}{\partial \eta} \right|_w \quad (9)$$

where the wall mass fraction gradient can be evaluated from the surface and flowfield solution. Finally, with the elemental composition and the elemental diffusive mass flux at wall, the mass blowing rate can be evaluated using Eq.(6). Among the N_{el} equations of this type there are $N_{el} - 1$ relations due to the fact that the elemental compositions of the atmosphere and of the surface material are known; the only unknown is their relative amount at the wall. Therefore the mass blowing rate can be obtained from Eq.(6) using any of the elements of the system.

During the computational transitory the mass blowing rate boundary condition and the wall chemical composition are continuously updated until the steady-state condition is reached. Mass blowing rate must be updated continuously because it depends on the boundary layer solution (via the diffusive mass fluxes) and at the same time it affects its development. When steady-state is reached, the mass blowing rate is everywhere consistent with the mass balance Eq.(2) and the wall composition is in chemical equilibrium with the wall material at the wall pressure and temperature. Unlike the *thermochemical table* model, the mass balance equation is not inserted in the chemical tables but is part of the solver's boundary conditions, through Eq.(6), and thus no simplified mass transfer model has to be introduced.

3. Results

The fully-coupled procedure described above is applied to a flat plate made of pure carbon (graphite). Isothermal solutions with different surface temperatures are presented to examine their effects on flow predictions. Chemical reactions between the wall material and the environmental gas are considered only at the surface using an equilibrium approach. Once the wall composition has been calculated, the species are not allowed to react as they are diffusing across the boundary layer. For the present calculations, the thermodynamic and transport properties of the single species are described by curve fits.⁸ Mixture properties for conductivity and viscosity are derived from the Wilke's rule. The diffusion model used is limited to binary diffusion using a constant Lewis number.

3.1 Supersonic flat plate with fully-coupled ablation model

The supersonic ($M = 4$) flow of air over a graphite flat plate is analyzed. Three different surface temperatures are considered: a) $T_w = 2500$ K; b) $T_w = 3800$ K; and c) $T_w = 3900$ K. The environmental gas is frozen air with equilibrium composition at the freestream thermodynamic state ($p = 1$ bar, $T = 4000$ K, $y_{N_2} = 0.767$, $y_O = 0.233$). The equilibrium composition between gas phase and solid phase is imposed; two ablation species are considered (CO and C_3) which make up more than 85% of the equilibrium mixture for the actual conditions of pressure and temperature. Species with minor concentrations have been neglected.

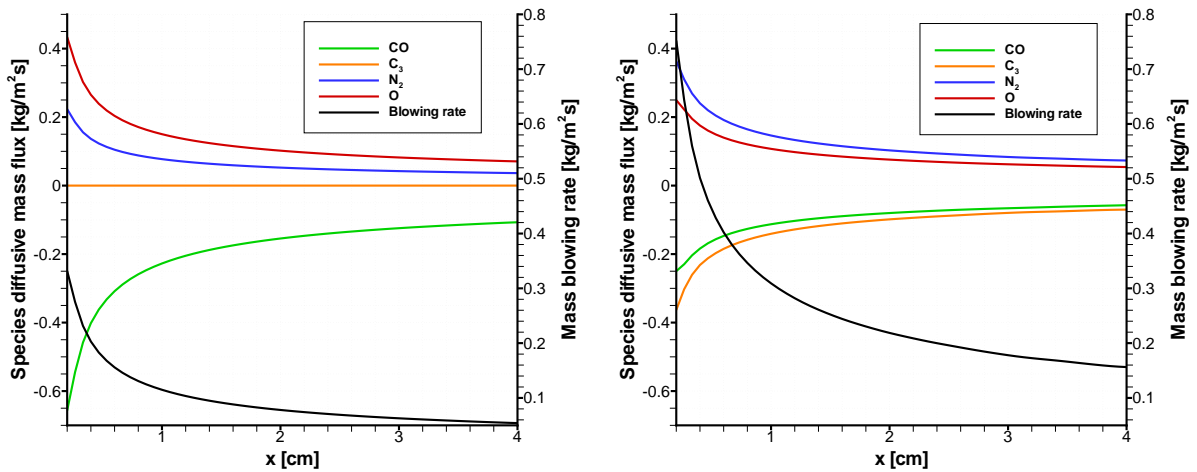


Figure 2: Species diffusion mass fluxes and mass blowing rate for $T_w = 2500$ K (left) and $T_w = 3800$ K (right).

Figure 2 shows the wall diffusive mass flux of each species (CO , C_3 , N_2 , O) together with the mass blowing rate. According to the surface mass balance Eq.(2), the mass blowing rate is determined by the wall diffusive mass flux, together with the surface and material composition. Mass blowing rate is thus strongly varying in the streamwise direction according to the growth of the boundary layer: higher mass blowing rates are experienced near the leading edge

of the plate where the diffusional mass fluxes are higher. The diffusional mass fluxes are positive for the atmospheric species and negative for the ablation products created at the surface. The surface temperature of 2500 K is too low to trigger surface sublimation (with formation of C_3) and the only ablation mechanism is the oxidation of carbon.

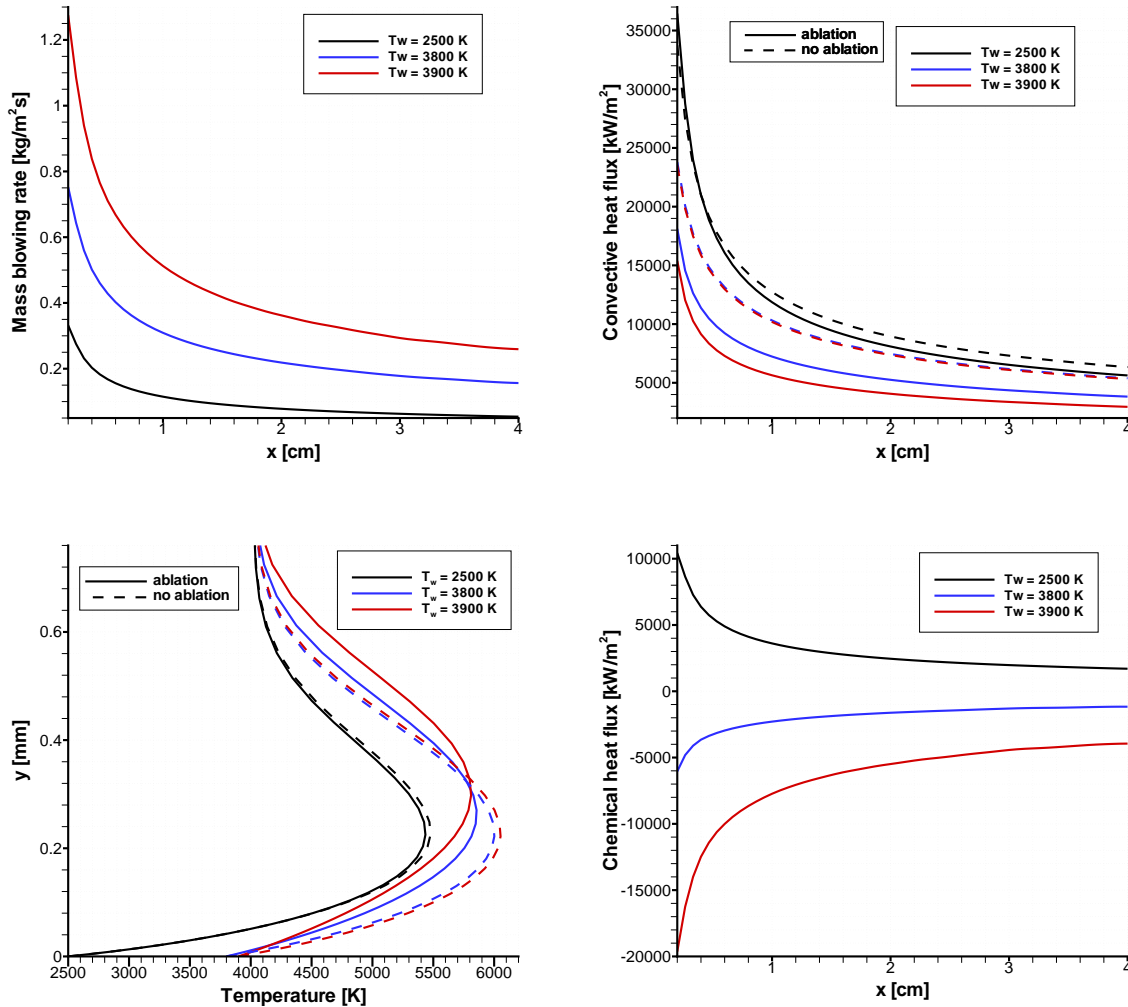


Figure 3: Mass blowing rate (up left), conductive heat flux (up right), temperature profile (down left), and chemical heat flux (down right) for three wall temperatures.

Figure 3 shows the mass blowing rate, surface conductive heat flux ($k \cdot \partial T / \partial \eta$), and surface chemical heat flux. All these variables are strongly varying with the surface temperature. The mass blowing rate increases with temperature, especially in the sublimation regime ($T_w = 3800$ K and $T_w = 3900$ K). In this regime, a slight increase of the surface temperature causes a large increase of the mass blowing rate. This behaviour has been previously shown by the sudden increase of B' with temperature in the thermochemical table model (Fig. 1). The surface heat flux is reduced due to the increase of wall temperature and mainly due to the so called *blockage effect* caused by the blowing of ablation product. The dashed lines in Fig. 3 (up right and down left) represent the same solution without ablation. The effect of *blockage* is evident in the sublimation regime where the heat flux is highly reduced if compared to the non-ablating case. The blowing of ablation products thus generates a cooling of the boundary layer which consequently reduces the wall heat flux. This can be seen looking at the temperature profiles shown in Fig. 3 (down left). For strong blowing the blockage effect is one of the major mechanism to limit the temperature rise inside the material. Finally, Fig. 3 (down right) shows the *chemical heat flux* for the three cases. It can be seen that in the oxidation regime ($T_w = 2500$ K) the chemical flux is positive, while in the sublimation regime it is negative. Therefore in the former regime the chemical reactions at wall are releasing heat, whereas in the latter they are absorbing it. This is due to the fact that the oxidation reaction of graphite (with formation of CO) is an exothermic process whereas the vaporization process (with formation of C_3) is

endothermic.

3.2 Comparison with thermochemical table approaches

With the procedure developed in this work, the mass balance equation is solved inside the CFD code, through the boundary condition. However, in many cases CFD codes are loosely coupled with the material and often the flowfield solutions are obtained using ablating boundary conditions with B' tables or even non-ablating boundary conditions corrected with blowing reduction equations.

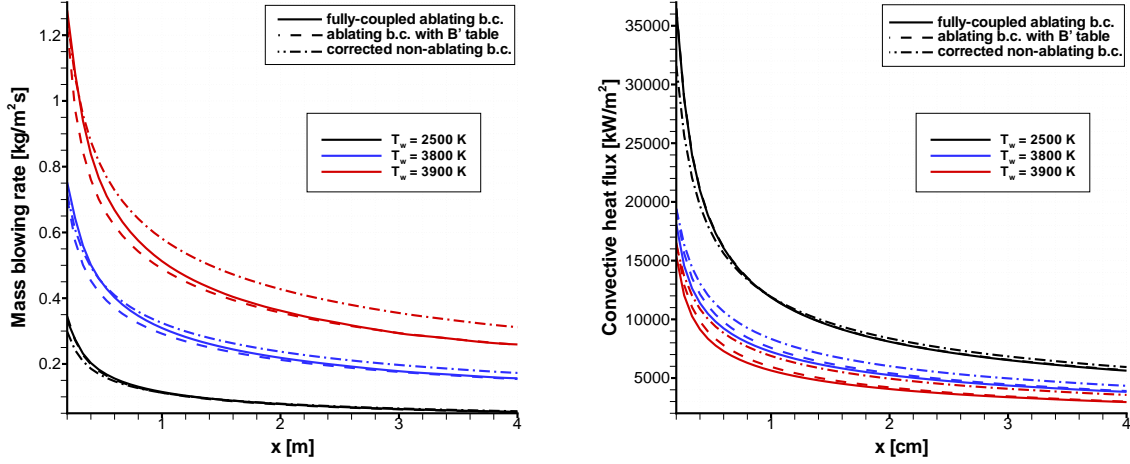


Figure 4: Mass blowing rate (left) and conductive heat flux (right) for different wall temperatures with three different boundary conditions.

When a *thermochemical table* approach is used, the mass blowing rate is obtained by tables such as those in Fig. 1 (left); the diffusion coefficient C_m is derived from semi-empirical relations such as⁹:

$$C_m = C_h \cdot Le^{-2/3} \quad (10)$$

where C_h is the heat transfer coefficient and is evaluated from the CFD solution by its definition¹⁰:

$$C_h = \frac{k \left. \frac{\partial T}{\partial \eta} \right|_w}{\rho_e u_e (h_r - h_{e,w})} \quad (11)$$

where h_r is the recovery enthalpy and $h_{e,w}$ is the enthalpy of the edge gas at the wall temperature. Eq.(11) is used to evaluate the heat transfer coefficient from the CFD solution and C_h is then used with Eq.(10) to compute C_m . With C_m and the B' value coming from the table, the mass blowing rate can be finally evaluated.

When *non-ablating boundary conditions* are used (no mass injection and no chemical reactions at wall), a blowing correction is typically adopted to reduce the computed heat flux to take into account of the blockage effect due to the ablation gases injected into the boundary layer. The most commonly used blowing-correction equation is¹⁰:

$$C_h = C_{h_0} \left[\frac{\ln(1 + 2\lambda \dot{m} / (\rho_e u_e C_h))}{2\lambda \dot{m} / (\rho_e u_e C_h)} \right] = C_{h_0} \left[\frac{\ln(1 + 2\lambda B' Le^{-2/3})}{2\lambda B' Le^{-2/3}} \right] \quad (12)$$

where λ is a blowing reduction parameter; with $\lambda = 0.5$ Eq.(12) reduces to the classical laminar-flow blowing correction. When a non-ablating CFD solution is performed, Eq.(11) is used to compute the non-ablative heat transfer coefficient C_{h_0} which is then reduced with the use of Eq.(12). The corrected C_h is finally used to evaluate the mass blowing rate as in the case of thermochemical table approach with ablating boundary conditions.

Fig. 4 shows the mass blowing rate and conductive heat flux for the three wall temperatures, computed with three different boundary conditions: fully-coupled ablating boundary conditions, ablating boundary conditions coupled

with $F(T, p, B')$ thermochemical tables, and non-ablating boundary conditions coupled with thermochemical tables and blowing correction equation. Both the blowing rate and the heat flux clearly show the error introduced by the simplified boundary conditions. The agreement between the table approach and the fully-coupled approach is very good at the lowest temperature but gets worse as the temperature and consequently the mass blowing rate are increased. Obviously the non-ablating approach is the one leading to major errors. The comparison between the cases with ablating boundary conditions shows that at the higher surface temperatures the table-predicted mass blowing rate and heat flux are affected by a certain degree of inaccuracy. These results show the limitations of the *thermochemical-table* approaches due to the simplified boundary-layer diffusion model expressed by Eq.(7), which was developed⁷ from the laminar boundary-layer theory over flat plates; thus the present comparisons between the two approaches are made in the most favourable condition. For turbulent solutions over more complex geometries the error is expected to be definitely larger.

4. Conclusions

A general surface boundary condition with mass balance for an ablating surface has been derived assuming equilibrium between the gas and the solid phase. A computer procedure based on these surface conditions was developed and integrated with a two-dimensional axisymmetric full Navier-Stokes equation solver coupled with an equilibrium ablation model. Solutions with various surface boundary conditions were obtained to study the effects on surface composition and ablation rate. The effect of gas injection in the boundary layer is studied focusing the attention on the wall heat flux and its reduction due to the ablation phenomenon. Results have been compared with the most commonly adopted approaches and the inaccuracy of simpler methodologies has been shown.

5. Acknowledgments

This study was performed in the frame of the TRP (Technology Research Programme) on *Multiphysics Modeling of Near Surface Phenomena* Contract No. 19168/05/NL/IA with the European Space Agency ESA-ESTEC Centre.

References

- [1] Milos F. S., Rasky D. J., Review of Numerical Procedures for Computational Surface Thermochemistry, *Journal of Thermophysics and Heat Transfer*, Vol. 8, No. 1, Jan-March 1994.
- [2] Chen Y. K., Henline W. D., Hypersonic Nonequilibrium Navier-Stokes Solutions over an Ablating Graphite Nosedip, *Journal of Spacecraft and Rockets*, Vol. 31, No. 5, Sept-Oct 1994.
- [3] Nasuti F., Onofri M., Analysis of Unsteady Supersonic Viscous Flows by a Shock Fitting Technique, *AIAA Journal*, Vol. 34, No. 7, July 1996, pp. 1428-1434.
- [4] Martelli E., Studio della Fluidodinamica Interna di Ugelli Propulsivi di Tipo Dual Bell, PhD Thesis, Dept. of Mechanics and Aeronautics, Univ. of Rome "La Sapienza", Rome, Italy, 2005 (in Italian).
- [5] Moretti G., A Technique for Integrating Two-Dimensional Euler Equations, *Computer and Fluids*, Vol. 15, No.1, 1987, pp. 59-75.
- [6] Zhlukov S. V., Takashi A., Viscous Shock-Layer Simulation of Airflow past Ablating Blunt Body with Carbon Surface, *Journal of Thermophysics and Heat Transfer*, Vol. 13, No. 1, 1999.
- [7] Kendall R. M., Rindal R. A., An Analysis of the Chemically Reacting Boundary Layer and Charring Ablator. Part V: A General Approach to the Thermochemical Solution of Mixed Equilibrium-Nonequilibrium, Homogeneous or Heterogeneous Systems, *NASA CR-1064*, June 1968.
- [8] Gordon S., McBride B. J., Computer Program for Calculation of Complex Chemical Equilibrium Compositions and Applications, *NASA RP-1311*, October 1994.
- [9] Spalding D. B., Convective Mass Transfer, an Introduction, *Edward Arnold*, London, 1963.
- [10] Chen Y. K., Milos F. S., Two-Dimensional Implicit Thermal Response and Ablation Program for Charring Materials, *Journal of Spacecraft and Rockets*, Vol. 38, No. 4, July-August 2001.



This page has been purposely left blank